

---

LHC Run-2 bounds on the  $Z'$  boson mass  
in Classically Conformal  $U(1)'$  extended SM  
with EW Vacuum Stability

Dai-suke TAKAHASHI (OIST)

Okinawa Institute of Science and Technology Graduate University

Phys. Rev. D 93, 115038 (2016)

Phys. Rev. D 92, 015026 (2015)

In collaboration with

A. DAS (U. of Alabama), S. ODA (OIST) and N. OKADA (U. of Alabama)

# Motivation

---

## 1. Gauge hierarchy problem

- ▶ No SUSY particle so far
- ▶ An alternative : Coleman-Weinberg mechanism ['73]

Classically Conformal Invariance + Quantum Correction



Massless Lagrangian @ Tree level



Mass generation

## 2. C.W. mechanism for SM ?

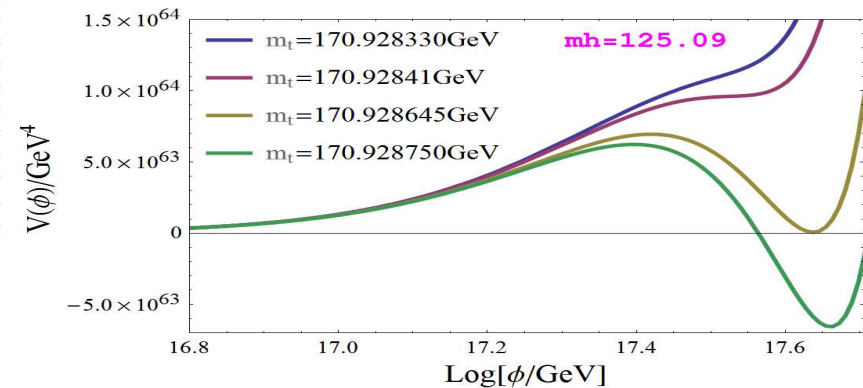
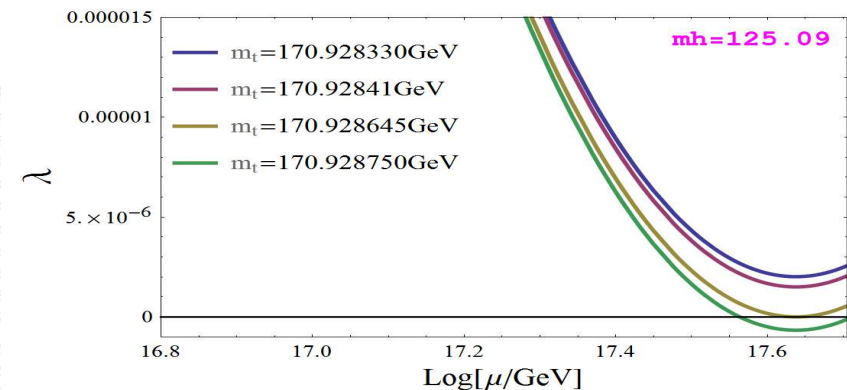
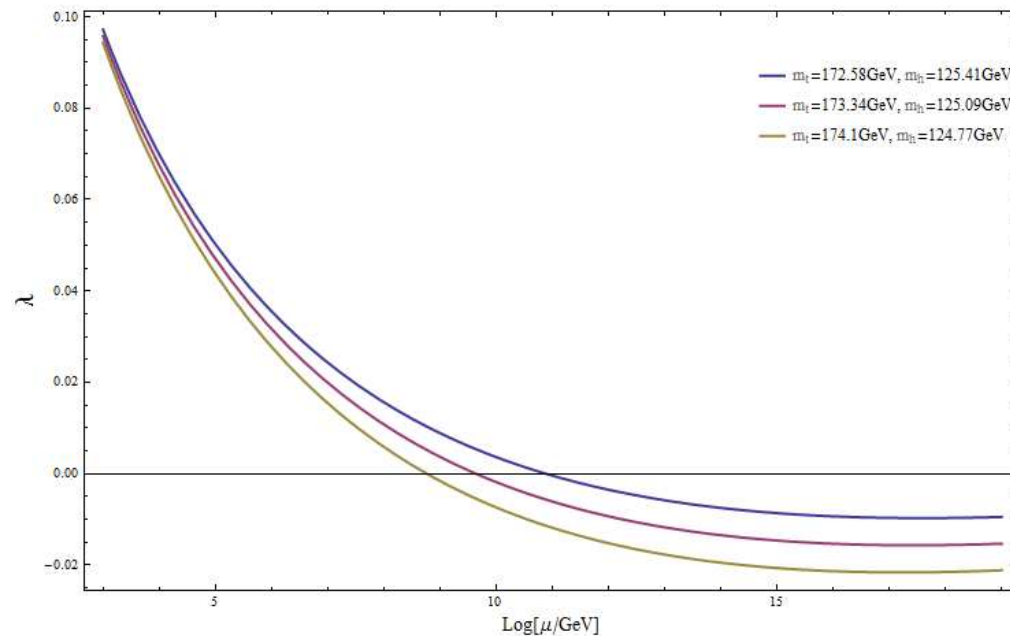
- ▶ Too large  $m_t$  [173 GeV] for C.W.
  - > SM Higgs field is unbounded below ['79 Fujikawa]
- ▶ Extension is needed for C.W.
  - > ex. )  $U(1)_{B-L}$  extension ['09 Iso, Okada, Orikasa]



### 3. Higgs discovery and its vacuum instability

- ▶ Top quark mass:  $173.34 \pm 0.76$  GeV [2014 March, Tevatron and LHC]
- ▶ Higgs mass:  $125.09 \pm 0.21(\text{stat.}) \pm 0.11(\text{syst.})$  GeV

[2015 March, ATLAS and CMS]

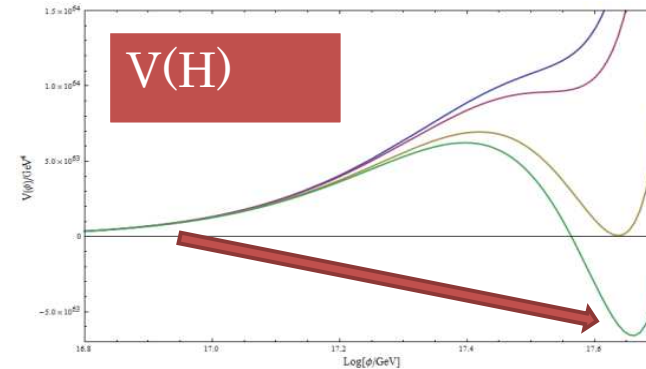


- ▶ we used the data of 2014 for the Higgs mass 125.03 GeV [‘15 S. Oda, N. Okada, D.T.]

# Motivation

## 3. LHC results

[ Higgs Mass + Top Quark Mass ]

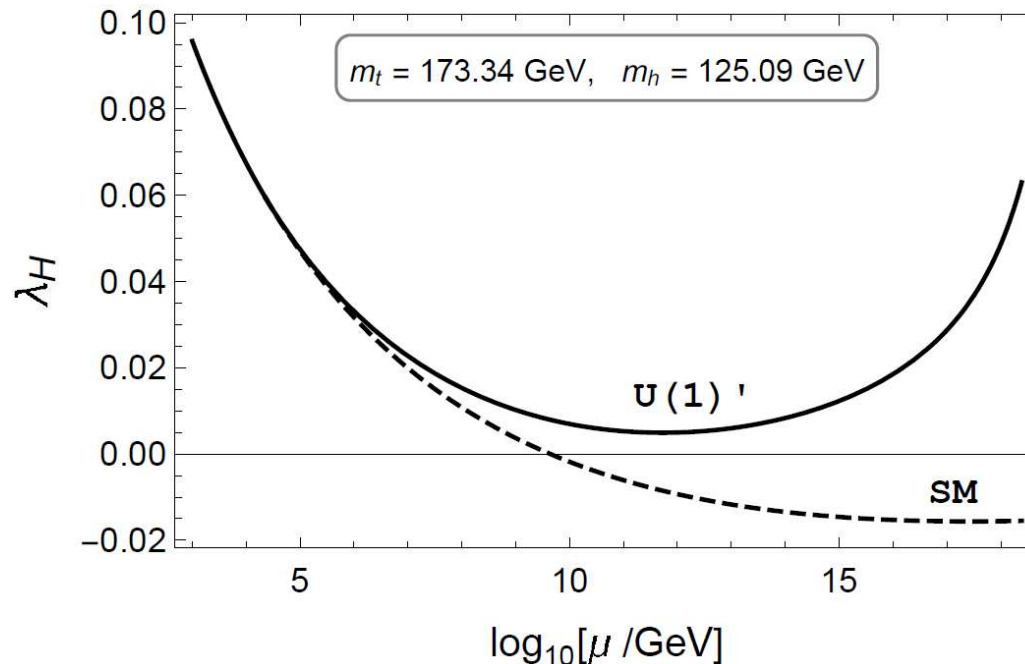


1D potential

- ▶ SM has negative Higgs quartic coupling  $\lambda$  at high energy scale.  
(cf.  $U(1)_{B-L}$  has also same situation.)
- ▶ It might not be a problem,  
if a Vacuum Transitional time ( $\tau = 1/\Gamma_{\text{false} \rightarrow \text{true}}$ )  $>$  a Lifetime of the Universe.
- ▶ What is the Shape of 2 Fields Effective Potential  $V_{\text{eff}}(H, \Phi)$  in Extended Models?
  - > Flat direction toward the true vacuum [Problem] ?

# Solving instability by General U(1) extension

## 4. “General” U(1) extension + C.W. [‘15 S. Oda, N. Okada, D. Takahashi]



- ▶ Non-negative  $\lambda$  coupling at all energy scale [Higgs vacuum is stable]
- ▶ Testable TeV scale  $Z'$  boson @ LHC
- ▶ Providing “Gauge Hierarchy”, “Mass Origin”,  
“EW sym. breaking”, and “Tiny neutrino mass”



$U(1)'$ : linear combination  $U(1)_Y + U(1)_{B-L}$

# 1. The model Classically Conformal $SU(3)_c \times SU(2)_L \times U(1)_Y \times U(1)'$

	$SU(3)_c$	$SU(2)_L$	$U(1)_Y$	$U(1)'$ [15 S. Oda, N. Okada, and D. Takahashi]	
$q_L^i$	<b>3</b>	<b>2</b>	$+1/6$	$x_q =$	$\frac{1}{3}x_H + \frac{1}{6}x_\Phi$
$u_R^i$	<b>3</b>	<b>1</b>	$+2/3$	$x_u =$	$\frac{4}{3}x_H + \frac{1}{6}x_\Phi$
$d_R^i$	<b>3</b>	<b>1</b>	$-1/3$	$x_d =$	$-\frac{2}{3}x_H + \frac{1}{6}x_\Phi$
$\ell_L^i$	<b>1</b>	<b>2</b>	$-1/2$	$x_\ell =$	$-x_H - \frac{1}{2}x_\Phi$
$\nu_R^i$	<b>1</b>	<b>1</b>	$0$	$x_\nu =$	$-\frac{1}{2}x_\Phi$
$e_R^i$	<b>1</b>	<b>1</b>	$-1$	$x_e =$	$-2x_H - \frac{1}{2}x_\Phi$
$H$	<b>1</b>	<b>2</b>	$+1/2$	$x_H =$	$x_H$
$\Phi$	<b>1</b>	<b>1</b>	$0$	$x_\Phi =$	$x_\Phi$

$(x_H, x_\phi) = (0, 2)$   
 $\Rightarrow U(1)_{B-L}$   
 $(x_H, x_\phi) = (\frac{1}{2}, 0)$   
 $\Rightarrow U(1)_Y$   
 $(x_H, x_\phi) = (-1, 2)$   
 $\Rightarrow U(1)_R$   
 $(x_H, x_\phi) = (-\frac{16}{41}, 2)$   
 $\Rightarrow$  Orthogonal

$$D_\mu \supset \partial_\mu - i \left( Y_1 \begin{matrix} Y_X \end{matrix} \right) \begin{pmatrix} g_1 & \begin{matrix} g_{1X} \end{matrix} \\ \begin{matrix} g_{X1} \end{matrix} & g_X \end{pmatrix} \begin{pmatrix} B_\mu \\ \begin{matrix} B'_\mu \end{matrix} \end{pmatrix}$$

where  $Y_1$  ( $Y_X$ ) are  $U(1)_Y$  ( $U(1)'$ ) charge of a particle,

and  $g_{X1}$  and  $g_{1X}$  are kinetic mixings between the two  $U(1)$  gauge bosons.

$$\mathcal{L}_{Yukawa} = -Y_u^{ij} \bar{q}_L^i u_R^j \tilde{H} - Y_d^{ij} \bar{q}_L^i d_R^j H - Y_\nu^{ij} \bar{\ell}_L^i \nu_R^j \tilde{H} - Y_e^{ij} \bar{\ell}_L^i e_R^j H - Y_M^i \bar{\nu}_R^{ic} \nu_R^i \Phi + \text{h.c.}$$

## 2. Radiative U(1)' symmetry breaking

---

- ▶ Classically conformal symmetry

$$V = \lambda_H (H^\dagger H)^2 + \lambda_\Phi (\Phi^\dagger \Phi)^2 + \lambda_{mix} (H^\dagger H) (\Phi^\dagger \Phi)$$

- ▶ Coleman-Weinberg potential at 1-loop level

\* Assuming the mixing between two Higgs sectors are small,  
we first consider U(1)' sector.

$$V(\phi) = \frac{\lambda_\Phi}{4} \phi^4 + \frac{\beta_{\lambda_\Phi}}{8} \phi^4 \left( \ln \left[ \frac{\phi^2}{v_\phi^2} \right] - \frac{25}{6} \right)$$

$$\phi/\sqrt{2} = \Re[\Phi] \qquad \beta_\Phi \simeq \frac{1}{16\pi^2} \left[ 6 (x_\Phi g_X)^4 - 16 \sum_i (Y_M^i)^4 \right]$$

---

▶  $\beta_\Phi = \frac{1}{16\pi^2} \left[ 20\lambda_\Phi^2 + 6x_\Phi^4 (g_{X1}^2 + g_X^2)^2 - 16 \sum_i (Y_M^i)^4 \right], \quad \lambda_\Phi^2 \ll (x_\Phi g_X)^4, \quad g_{1X} = g_{X1} = 0 \text{ at } \langle \phi \rangle = v_\phi$

### 3. Radiative U(1)' symmetry breaking (cont'd)

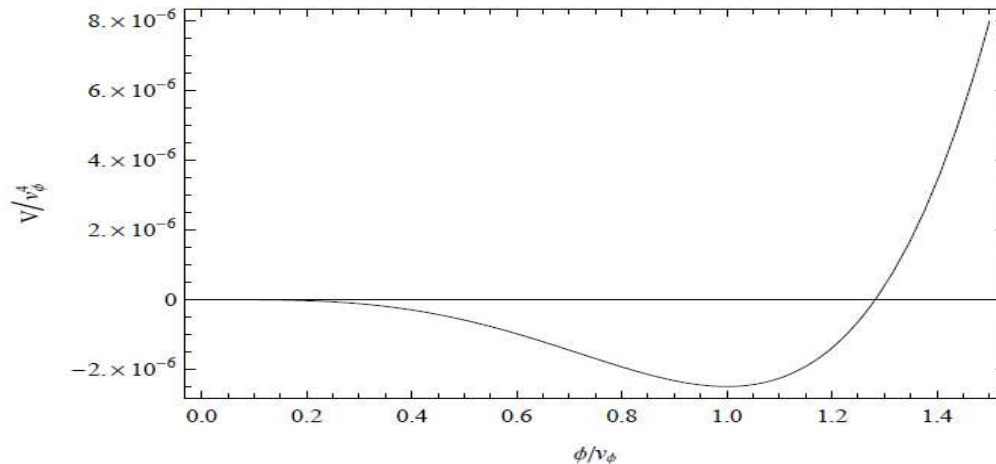
$$V(\phi) = \frac{\lambda_\Phi}{4}\phi^4 + \frac{\beta_{\lambda_\Phi}}{8}\phi^4 \left( \ln \left[ \frac{\phi^2}{v_\phi^2} \right] - \frac{25}{6} \right)$$

Renormalization condition of  $\lambda_\Phi$

Stationary condition that the potential realizes a minimum at  $\langle \phi \rangle = v_\phi$  leads to

$$\left. \frac{dV}{d\phi} \right|_{\phi=v_\phi} = 0 \quad \Rightarrow \quad \lambda_\Phi = \frac{11}{6}\beta_{\lambda_\Phi} \quad \text{Connected } \lambda_\Phi \text{ with } g_X$$

U(1)' symmetry is broken by radiative corrections



$$\beta_\Phi \simeq \frac{1}{16\pi^2} \left[ 6(x_\Phi g_X)^4 - 16 \sum_i (Y_M^i)^4 \right]$$



## 4. Mass spectrum

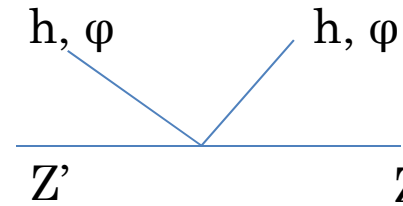
---

U(1)' sym. breaking



- ▶ The U(1)' gauge boson (Z' boson)

$$m_{Z'} = \sqrt{(x_\Phi g_X v_\phi)^2 + (x_H g_X v_h)^2} \simeq x_\Phi \underline{g_X} v_\phi$$



•  $\mathcal{L}_{scalar} \supset (D\Phi)^\dagger (D\Phi)$

- ▶ The right-handed Majorana neutrinos

$$m_{Ni} = \sqrt{2} \underline{Y_M^i} v_\phi$$

•  $\mathcal{L}_{Yukawa} \supset -Y_M^i \bar{\nu}_R^{ic} \nu_R^i \Phi + h.c.$

- ▶ The U(1)' Higgs boson

$$m_\phi^2 = \left. \frac{d^2 V}{d\phi^2} \right|_{\phi=v_\phi} = \beta_\Phi v_\phi^2 \simeq \frac{3}{8\pi^2} ((x_\Phi g_X)^4 - 8y_M^4) v_\phi^2 \simeq \frac{3}{8\pi^2} \frac{m_{Z'}^4 - 2m_N^4}{v_\phi^2} > 0$$

•  $V(\phi) = \frac{\lambda_\Phi}{4} \phi^4 + \frac{\beta_\Phi}{8} \phi^4 \left( \ln \left[ \frac{\phi^2}{v_\phi^2} \right] - \frac{25}{6} \right)$

▶  $x_\Phi v_\phi \gg x_H v_h$

$\lambda_\Phi = \frac{1}{3!} \left. \frac{d^4 V(\phi)}{d\phi^4} \right|_{\phi=v_\phi}$  : Renormalization condition

## 5. Electroweak (EW) symmetry breaking

- ▶ U(1)' sym. breaking naturally triggers EW sym. breaking

$$V = \lambda_H (H^\dagger H)^2 + \lambda_\Phi (\Phi^\dagger \Phi)^2 + \lambda_{mix} (H^\dagger H) (\Phi^\dagger \Phi)$$

U(1)' sym. breaking



$$V(h) = \frac{\lambda_H}{4} h^4 + \frac{\lambda_{mix}}{4} v_\phi^2 h^2$$

EW sym. breaking



$$m_h^2 = \left. \frac{d^2 V}{dh^2} \right|_{h=v_h} = |\lambda_{mix}| v_\phi^2 = 2\lambda_H v_h^2$$



$$|\lambda_{mix}(v_\phi)| = 2\lambda_H(v_\phi) \left( \frac{v_h}{v_\phi} \right)^2 : \lambda_{mix} \text{ boundary condition at } v_\phi$$

$$H = \frac{1}{\sqrt{2}} \begin{pmatrix} 0 \\ h \end{pmatrix}, \quad \Phi = \frac{1}{\sqrt{2}} \phi$$

$$\lambda_{mix} < 0$$

- ▶  $\lambda_H \sim 0.1$  and  $v_\phi \gtrsim 10$  [TeV] by LEP [hep-ex:0312023, hep-ph:0408098].  $|\lambda_{mix}| \leq 10^{-5}$

# 6. $\lambda_H$ : SM Higgs quartic running coupling

[Higgs vacuum **Instability** and Stability]

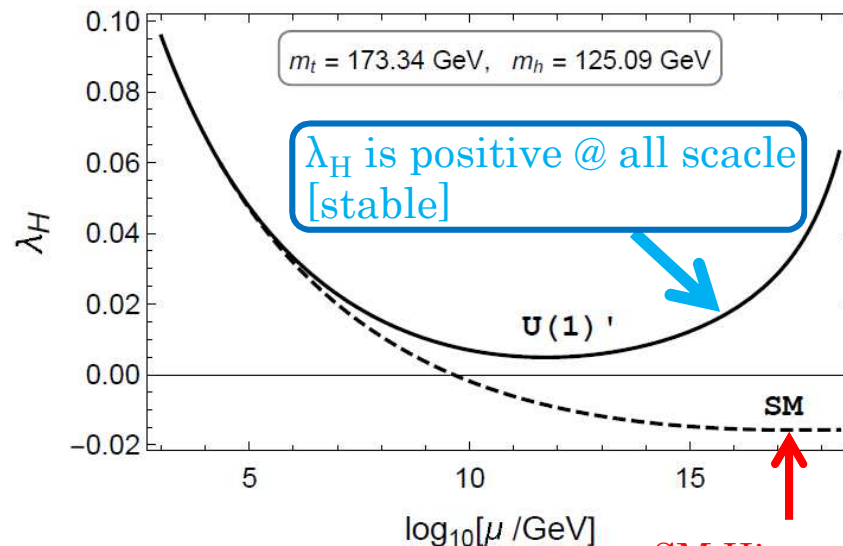
$$(x_H, x_\Phi) = (2, 2)$$

$$v_\Phi = 23 \text{ TeV}$$

$$g_X(v_\Phi) = 0.090$$

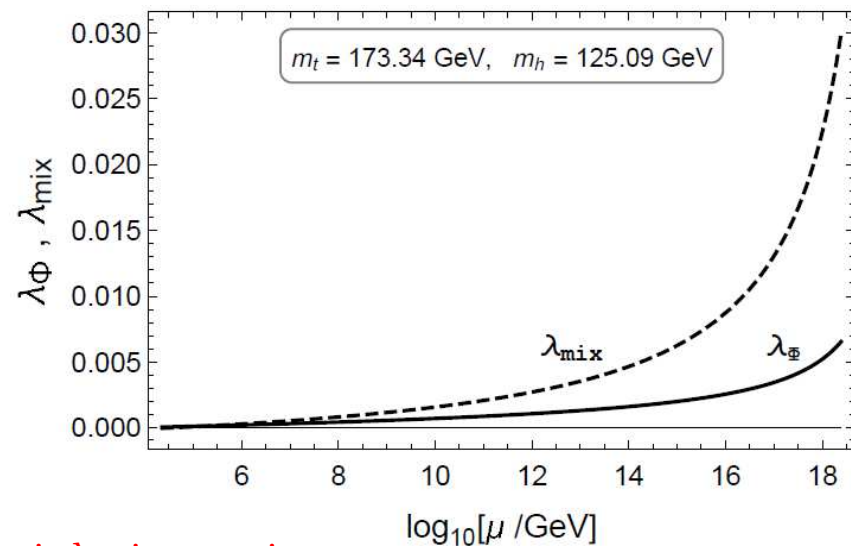
$$m_t = \underline{173.34 \text{ GeV}} \text{ [Tevatron and LHC, March 2014]}$$

$$m_h = \underline{125.09 \text{ GeV}} \text{ [ATLAS and CMS, Mar 2015]}$$



(a)

SM Higgs quartic  $\lambda_H$  is negative  
[unstable]



(b)

Figure 1: (a) The evolutions of the Higgs quartic coupling  $\lambda_H$  (solid line) for the inputs  $m_t = 173.34 \text{ GeV}$  and  $m_h = 125.09 \text{ GeV}$ , along with the SM case (dashed line). (b) The RG evolutions of  $\lambda_\Phi$  (solid line) and  $\lambda_{\text{mix}}$  (dashed line). Here, we have taken  $x_H = 2$ ,  $v_\phi = 23 \text{ TeV}$  and  $g_X(v_\phi) = 0.09$ .

► \*Connected the U(1)' RGEs to the SM RGEs at  $v_\phi$  (the U(1)' sym. breaking scale).

2-loop level

## 7. 3D Parameter Scan [free : $x_H, g_X, v_\phi$ ]

\* The U(1)' gauge coupling constant  $g_X$  always appears with  $x_\phi$  or  $X_H$ .  
---- > We fix  $x_\phi=2$  without loss of generality.

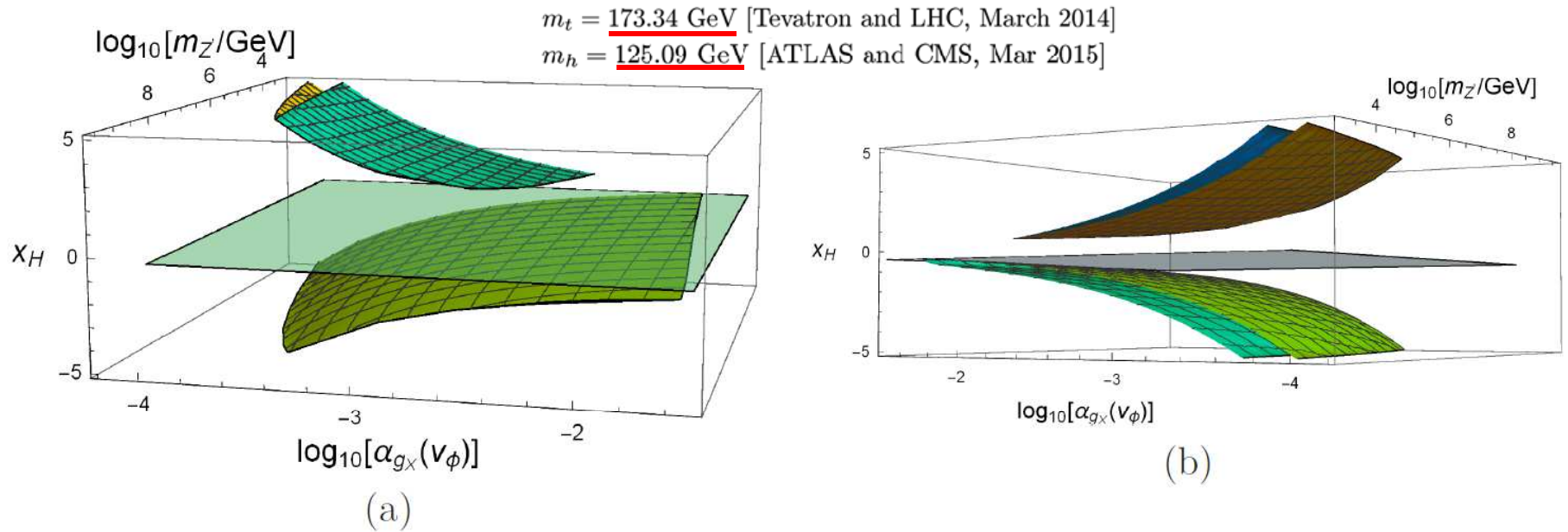


Figure 2: (a) The result of 3-dimensional parameter scans for  $v_\phi$ ,  $g_X$  and  $x_H$ , shown in  $(m_{Z'}(\text{GeV}), \alpha_{g_X}, x_H)$  parameter space with  $m_{Z'} \simeq x_\phi g_X v_\phi$ , by using the inputs  $m_t = 173.34 \text{ GeV}$  and  $m_h = 125.09 \text{ GeV}$ . As a reference, a horizontal plane for  $x_H = -16/41$  is shown, which corresponds to the orthogonal case. (b) Same 3-dimensional parameter scans as (a), but different angle.

\* The U(1)' gauge coupling constant  $g_X$  always appears with  $x_\phi$  or  $X_H$ .  
 ---- > We fix  $x_\phi=2$  without loss of generality.

## 8. 2D Parameter Scan ( $x_H, g_X, v_\phi$ )

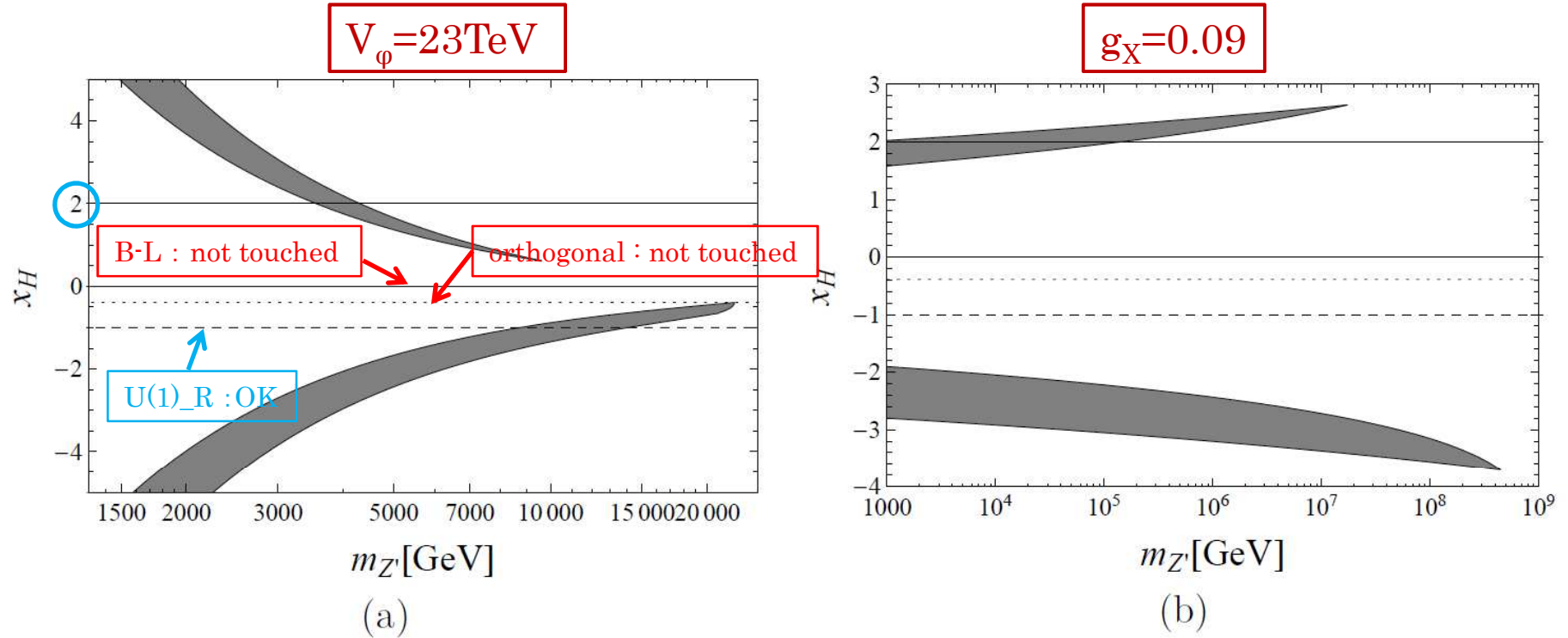


Figure 2: (a) The result of parameter scan for  $x_H$  and  $g_X$  with a fixed  $v_\phi = 23$  TeV, shown in  $(m_{Z'}, x_H)$ -plane with  $m_{Z'} = \sqrt{(x_\phi g_X v_\phi)^2 + (x_H g_X v_h)^2} \simeq x_\phi g_X v_\phi$ . As a reference, horizontal lines are depicted for  $x_H = 2$ ,  $0$  [U(1)<sub>B-L</sub> case],  $-16/41$  [orthogonal case], and  $-1$  [U(1)<sub>R</sub> case]. (b) Same as (a), but parameter scan for  $x_H$  and  $v_\phi$  with a fixed  $g_X = 0.09$ .

► Remark:  $m_{Z'} = \sqrt{(x_\phi g_X v_\phi)^2 + (x_H g_X v_h)^2} \simeq x_\phi g_X v_\phi$



## 9. LHC Run-2 bounds on $Z'$ mass

We calculate the dilepton production cross section for the process  $pp \rightarrow Z' + X \rightarrow \ell^+ \ell^- + X$ . The differential cross section with respect to the invariant mass  $M_{\ell\ell}$  of the final state dilepton is described as

$$\frac{d\sigma(pp \rightarrow \ell^+ \ell^- X)}{dM_{\ell\ell}} = \sum_{a,b} \int_{\frac{M_{\ell\ell}^2}{E_{\text{CM}}^2}}^1 dx_1 \frac{2M_{\ell\ell}}{x_1 E_{\text{CM}}^2} f_a(x_1, M_{\ell\ell}^2) f_b\left(\frac{M_{\ell\ell}^2}{x_1 E_{\text{CM}}^2}, M_{\ell\ell}^2\right) \hat{\sigma}(\bar{q}q \rightarrow \ell^+ \ell^-),$$

where  $f_a$  is the parton distribution function for a parton “a”, and  $E_{\text{CM}} = 13$  TeV (Run-2), or 8 TeV (Run-1), is the center-of-mass energy of the LHC. In our numerical analysis, we employ CTEQ5M for the parton distribution functions.

The cross section for the colliding partons with a fixed  $x_\Phi = 2$  is given by

$$\begin{aligned} \hat{\sigma}(\bar{u}u \rightarrow \ell^+ \ell^-) &= \frac{\pi \alpha_{gX}^2}{81} \frac{M_{\ell\ell}^2}{(M_{\ell\ell}^2 - m_{Z'}^2)^2 + m_{Z'}^2 \Gamma_{Z'}^2} (85x_H^4 + 152x_H^3 + 104x_H^2 + 32x_H + 4) \\ \hat{\sigma}(\bar{d}d \rightarrow \ell^+ \ell^-) &= \frac{\pi \alpha_{gX}^2}{81} \frac{M_{\ell\ell}^2}{(M_{\ell\ell}^2 - m_{Z'}^2)^2 + m_{Z'}^2 \Gamma_{Z'}^2} (25x_H^4 + 20x_H^3 + 8x_H^2 + 8x_H + 4), \end{aligned}$$

where the total decay width of  $Z'$  boson is given by

$$\Gamma_{Z'} = \frac{\alpha_{gX} m_{Z'}}{6} \left[ \frac{103x_H^2 + 86x_H + 37}{3} + \frac{17x_H^2 + 10x_H + 2 + (7x_H^2 + 20x_H + 4) \frac{m_t^2}{m_{Z'}^2}}{3} \sqrt{1 - \frac{4m_t^2}{m_{Z'}^2}} \right]$$

Here, we have neglected all SM fermion masses except for  $m_t$ , and assumed  $m_N^i > m_{Z'}/2$  for simplicity. By integrating the differential cross section over a range of  $M_{\ell\ell}$  set by the ATLAS and the CMS analysis, respectively, we obtain the cross section as a function of  $x_H$ ,  $\alpha_{gX}$  and  $m_{Z'}$ , which are compared with the lower bounds obtained by the ATLAS and the CMS collaborations.

C.C. U(1)' model

## 10. $Z'_{SSM}$ search [ATLAS]

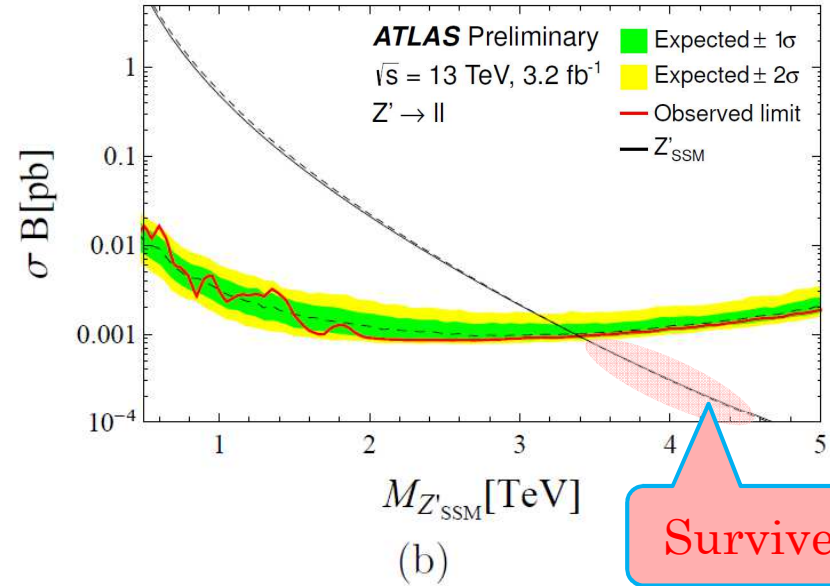
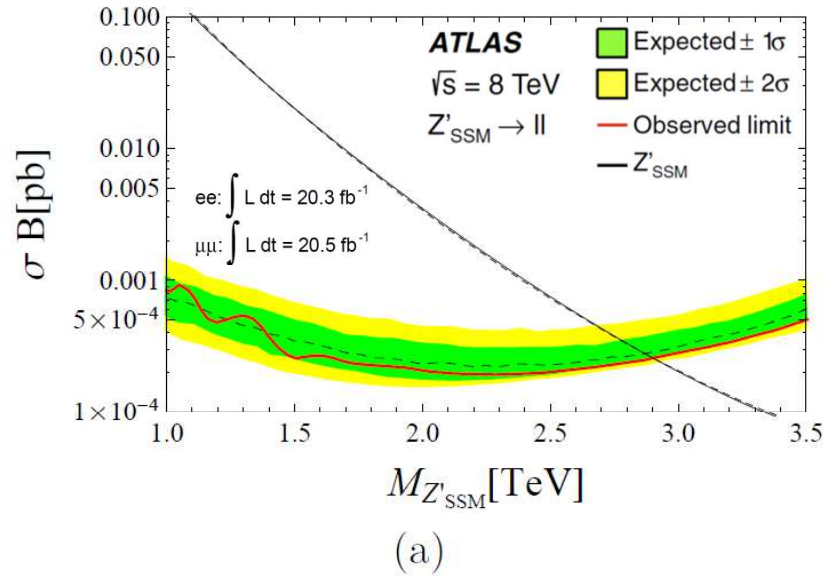


Figure 7: (a) The cross section as a function of the  $Z'_{SSM}$  mass (solid line) with  $k = 1.17760$ , along with the ATLAS (LHC Run-1 with  $\sqrt{s} = 8$  TeV) result in Ref. [16] from the combined dielectron and dimuon channels. (b) Same as (a), but with  $k = 1.19030$ , along with the ATLAS (LHC Run-2 with  $\sqrt{s} = 13$  TeV) result in Ref. [26]

## 10-2. $Z'_{SSM}$ search [CMS]

---

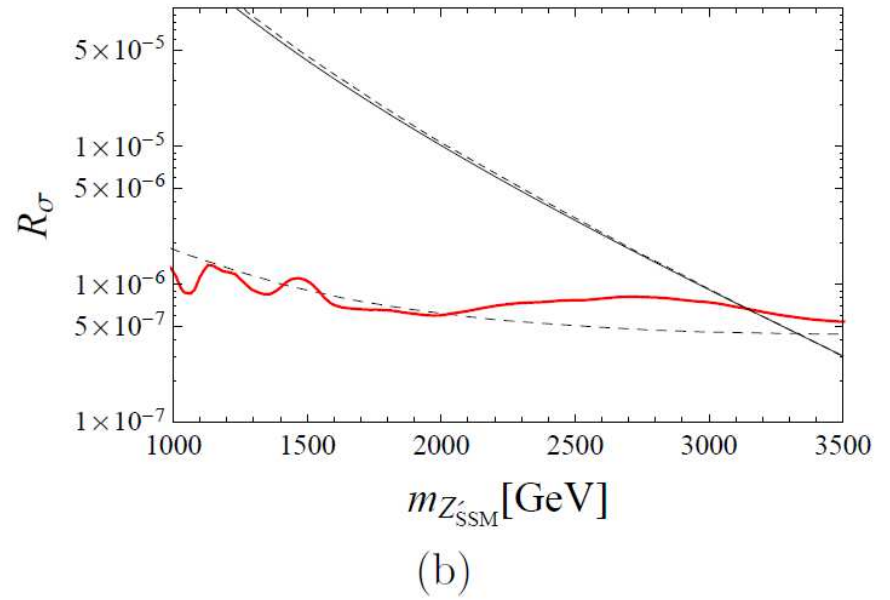
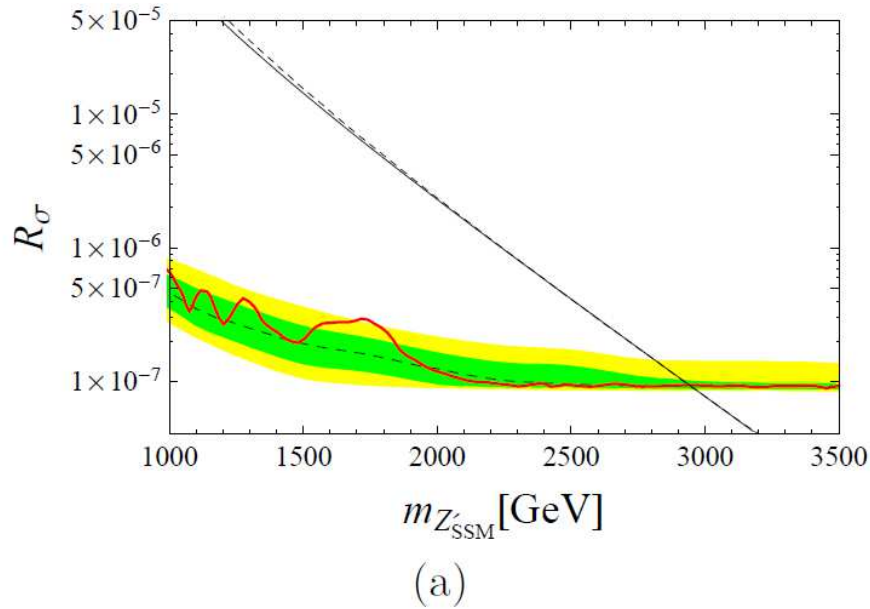


Figure 8: (a) The cross section as a function of the  $Z'_{SSM}$  mass (solid line) with  $k = 1.00507$ , along with the CMS (LHC Run-1 with  $\sqrt{s} = 8$  TeV) result in Ref. [17] from the combined dielectron and dimuon channels. (b) Same as (a), but with  $k = 1.64466$ , along with the CMS (LHC Run-2 with  $\sqrt{s} = 13$  TeV) result in Ref. [27]





# 11. Naturalness of the SM Higgs mass

Since the original theory is classically conformal and defined as a massless theory, the self-energy corrections to the SM Higgs doublet originates from corrections to the quartic coupling  $\lambda_{mix}$ . Thus, what we calculate to derive the naturalness bounds is quantum corrections to the term  $\lambda_{mix}h^2\phi^2$  in the effective Higgs potential.

$V_{\text{eff}}$  for  $h^2\Phi^2$  term

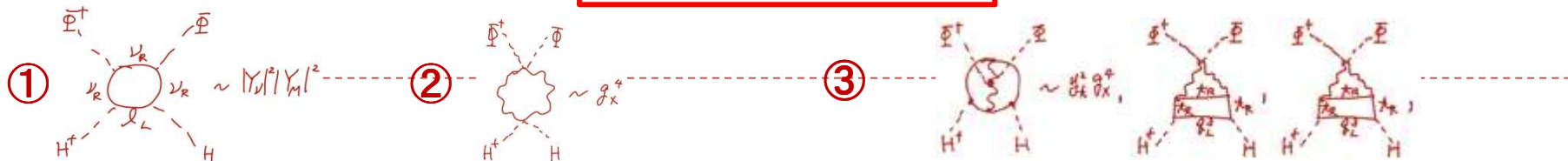
$$V_{\text{eff}} \supset \frac{\lambda_{mix}}{4}h^2\phi^2 + \frac{\beta_{\lambda_{mix}}}{8}h^2\phi^2 (\ln [\phi^2] + C), \quad (7.1)$$

where the logarithmic divergence and the terms independent of  $\phi$  are all encoded in  $C$ . Here, the coefficient of the major quantum corrections is given by

$$\beta_{\lambda_{mix}} \supset -\frac{48|Y_M|^2|Y_\nu|^2}{16\pi^2} + \frac{12x_H^2x_\Phi^2g_X^4}{16\pi^2} - \frac{4(19x_H^2 + 10x_Hx_\Phi + x_\Phi^2)x_\Phi^2y_t^2g_X^4}{(16\pi^2)^2}, \quad (7.2)$$

where ① the first term comes from the one-loop diagram involving the Majorana neutrinos, the ② second one is from the one-loop diagram involving the  $Z'$  boson, and the ③ third one is from the two-loop diagram involving the  $Z'$  boson and the top quark. By adding a counter term, we renormalize the coupling  $\lambda_{mix}$  with the renormalization condition,

$$\left. \frac{\partial^4 V_{\text{eff}}}{\partial h^2 \partial \phi^2} \right|_{h=0, \phi=v_\Phi} = \lambda_{mix}, \quad \text{Renormalization condition} \quad (7.3)$$



## 11-2. Naturalness of the SM Higgs mass

where  $\lambda_{mix}$  is the renormalized coupling. As a result, we obtain

$V_{\text{eff}}(h^2\Phi^2)$  term

$$V_{\text{eff}} \supset \frac{\lambda_{mix}}{4} h^2 \phi^2 + \frac{\beta_{\lambda_{mix}}}{8} h^2 \phi^2 \left( \ln \left[ \frac{\phi^2}{v_\Phi^2} \right] - 3 \right). \quad (7.4)$$

Renormalization condition

Substituting  $\phi = v_\phi$ , we obtain the SM Higgs self-energy correction as

$$\begin{aligned} \Delta m_h^2 &= -\frac{3}{4} \beta_{\lambda_{mix}} v_\phi^2 \quad \text{dominant} \\ &\sim \frac{9m_\nu m_N^3}{4\pi^2 v_h^2} - \frac{9}{4\pi} x_H^2 \alpha_{gX} m_{Z'}^2 + \frac{3m_t^2}{32\pi^3 v_h^2} (19x_H^2 + 20x_H + 4) \alpha_{gX} m_{Z'}^2 \end{aligned} \quad (7.5)$$

where we have used the seesaw formula,  $m_\nu \sim Y_\nu^2 v_h^2 / 2m_N$  [7], and set  $x_\Phi = 2$ . For the stability of the electroweak vacuum, we impose  $\Delta m_h^2 \lesssim m_h^2$  as the naturalness. For example, when the light neutrino mass scale is around  $m_\nu \sim 0.1$  eV, we have an upper bound from the first term of Eq. (7.5) for the Majorana mass as  $m_N \lesssim 3 \times 10^6$  GeV. This bound is much larger than the scale that we are interested in,  $m_N \lesssim 1$  TeV. The most important contribution to  $\Delta m_h^2$  is the second term of Eq. (7.5) generated through the one-loop diagram with the  $Z'$  gauge boson, and the third term becomes important in the case of  $U(1)_{B-L}$  model, because  $x_H = 0$  condition makes the second term vanished.

If  $\Delta m_h^2$  is much larger than the electroweak scale, we need a fine-tuning of the tree-level Higgs mass ( $|\lambda_{mix}|v_\Phi^2/2$ ) to reproduce the correct SM Higgs VEV,  $v_h = 246$  GeV. We simply evaluate a fine-tuning level as

Fine-tuning level

$$\delta = \frac{m_h^2}{2|\Delta m_h^2|}. \quad (7.6)$$

Here,  $\delta = 0.1$ , for example, indicates that we need to fine-tune the tree-level Higgs mass squared at the accuracy of 10% level. Some of finetuning levels are shown in Figs. 3, 4, 5(b) and 6(b), along with the results of parameter scans.

## 12-1. $Z'$ boson search ( $x_H, g_X, v_\phi=23\text{TeV}$ )

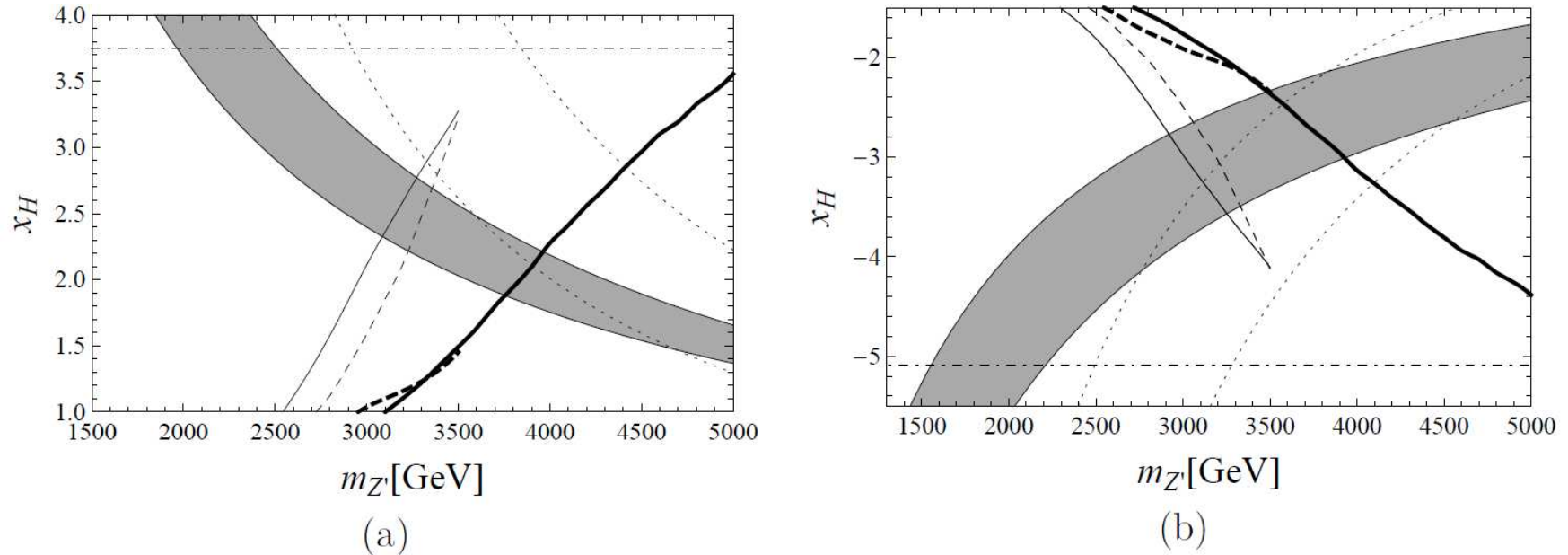


Figure 3: (a) The allowed positive  $x_H$  region at the TeV scale in Fig. 2(a) is magnified, along with the LEP bound (dashed-dotted line), the CMS Run1 bound (thin dashed line), the ATLAS Run1 bound (thin solid line), the CMS Run2 bound (thick dashed line) and the ATLAS Run2 bound (thick solid line) from direct search for  $Z'$  boson resonance. The region on the left side of the lines are excluded. Here, the naturalness bounds for 10% (right dotted line) and 30% (left dotted line) fine-tuning levels are also depicted. (b) Same as (a), but for negative  $x_H$  region.

► Remark:  $m_{Z'} = \sqrt{(x_\Phi g_X v_\phi)^2 + (x_H g_X v_h)^2} \simeq x_\Phi g_X v_\phi$



## 12-2. Z' boson search ( $x_H$ , $g_X=0.09$ , $v_\phi$ )

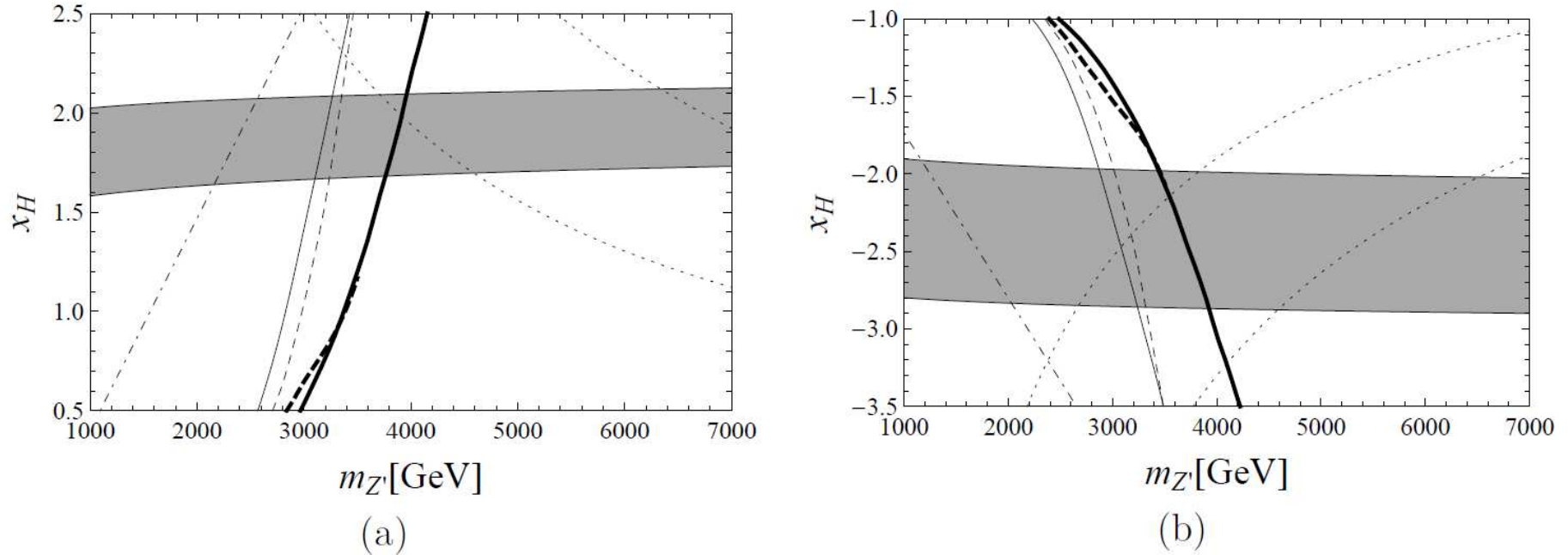
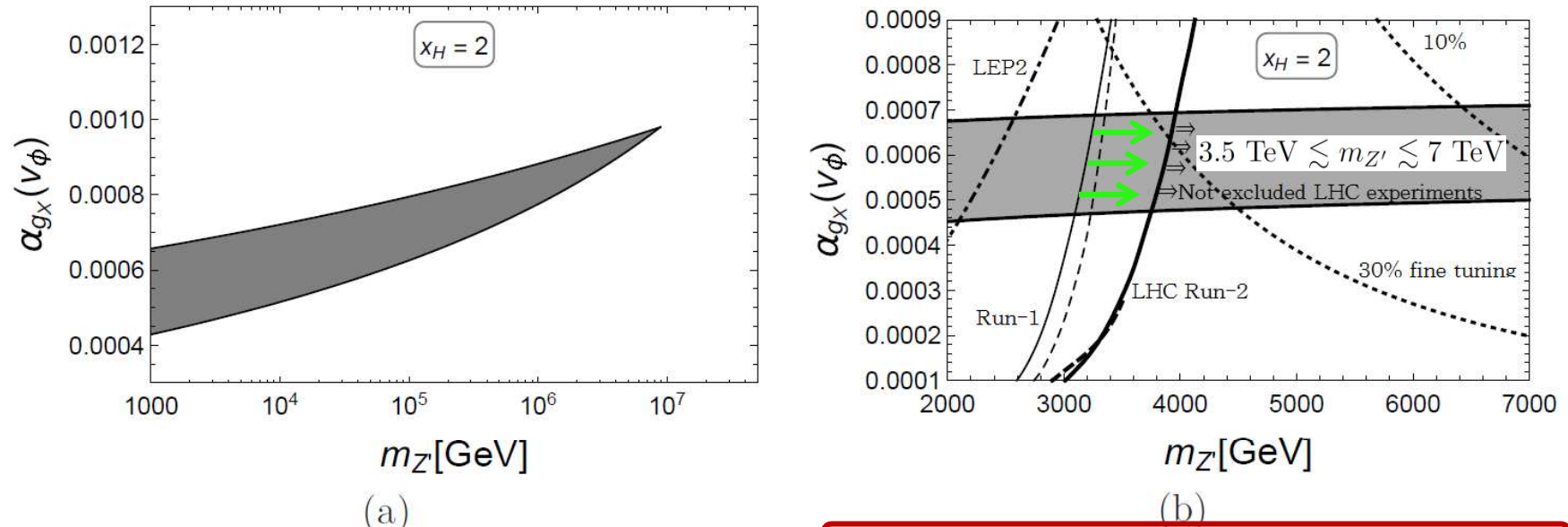


Figure 4: (a) The allowed positive  $x_H$  region at the TeV scale in Fig. 2(b) is magnified, along with the LEP bound (dashed-dotted line), the CMS Run1 bound (thin dashed line), the ATLAS Run1 bound (thin solid line), the CMS Run2 bound (thick dashed line) and the ATLAS Run2 bound (thick solid line) from direct search for  $Z'$  boson resonance. The region on the left side of the lines are excluded. Here, the naturalness bounds for 10% (right dotted line) and 30% (left dotted line) fine-tuning levels are also depicted. (b) Same as (a), but for negative  $x_H$  region.

► Remark:  $m_{Z'} = \sqrt{(x_\Phi g_X v_\phi)^2 + (x_H g_X v_h)^2} \simeq x_\Phi g_X v_\phi$

## 12-3. Z' boson search ( $x_H=2$ , $g_X$ , $v_\phi$ )



Run-2 bound is 500~600 GeV higher than RUN1 one.

Figure 6: (a) The result of parameter scan for  $v_\phi$  and  $g_X$  with a fixed  $x_H = 2$  in  $(m_{Z'}, \alpha_{g_X})$ -plane. (b) The allowed region at the TeV scale in (a) is magnified, along with the LEP bound (dashed-dotted line), the LHC Run-1 CMS bound (thin dashed line), the LHC Run-1 ATLAS bound (thin solid line), the LHC Run-2 CMS bound (thick dashed line) and the LHC Run-2 ATLAS bound (thick solid line) from direct search for  $Z'$  boson resonance. The region on the left side of the lines are excluded. Here, the naturalness bounds for 10% (right dotted line) and 30% (left dotted line) fine-tuning levels are also depicted.

► Remark:  $m_{Z'} = \sqrt{(x_\Phi g_X v_\phi)^2 + (x_H g_X v_h)^2} \simeq x_\Phi g_X v_\phi$

## 12-4. Z' boson search ( $x_H = -2.5$ , $g_X$ , $v_\phi$ )

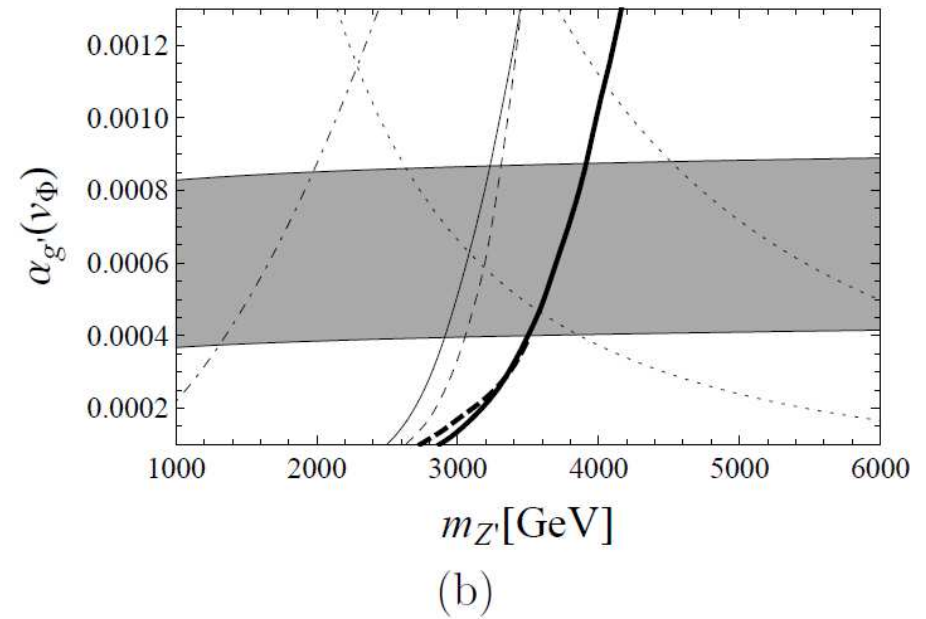
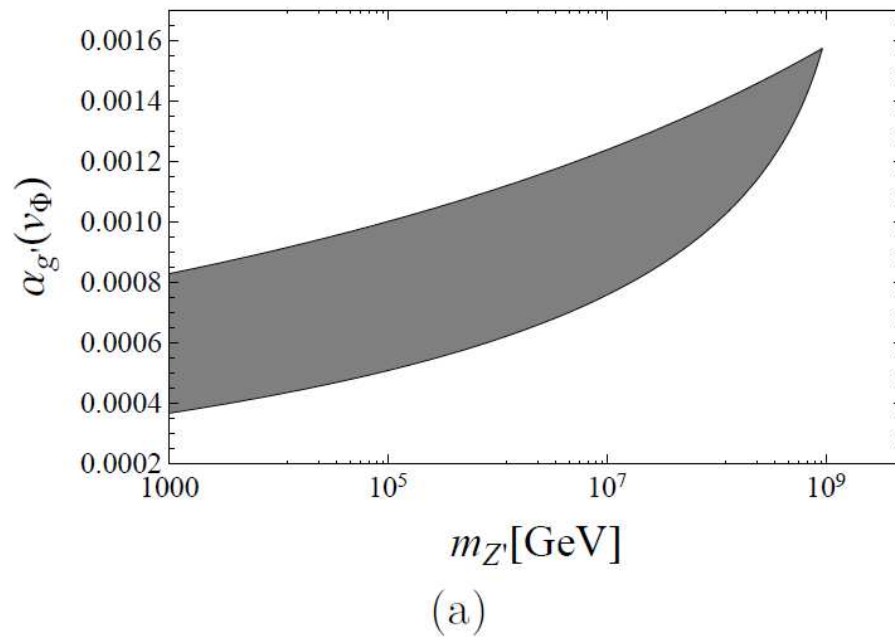


Figure 6: (a) Same as Fig. 5(a), but for  $x_H = -2.5$ . (a) Same as Fig. 5(b), but for  $x_H = -2.5$ .

► Remark:  $m_{Z'} = \sqrt{(x_\Phi g_X v_\phi)^2 + (x_H g_X v_h)^2} \simeq x_\Phi g_X v_\phi$

# 13. Summary and Conclusion

---

## 2-loop Classically conformal U(1)' extended SM

- ▶ New Particles in addition to the SM:
  - ▶ Complex scalar singlet ( $\Phi$ )  $\Leftarrow$  Seesaw, CW
  - ▶ Right-handed neutrinos ( $\nu_R$ ) [3 generations]  $\Leftarrow$  Neutrino Oscillation, Seesaw
  - ▶ U(1)' gauge boson ( $Z'$ )
- ▶ The model provides explanations to important issues in the SM:
  - ▶ [A] Gauge Hierarchy
  - ▶ [B] Origin of Mass [Dimensional Transmutation]
  - ▶ [C] Origin of EW Symmetry Breaking
  - ▶ [D] Tiny neutrino mass [seesaw mechanism]
  - ▶ [E] @ 2-loop level, more easily realize the SM Higgs vacuum stability

## Phenomenology and Run-2 results

- ▶ The model is also Testable @ LHC Run-2 with a 13-14 TeV
    - ▶ TeV scale new physics prediction with Naturalness
    - ▶ Radiative U(1)' sym. breaking naturally at TeV scale by C.W. mechanism
    - ▶  $Z'$  boson also naturally @ TeV scale
    - ▶ Run-2  $Z'$  boson mass bound is 500~600 GeV higher than Run1 one
- 





# THE END

---

## ***Thank you very much***

OIST Campus



OIST 沖縄科学技術大学院大学